CUESI: A Near Seafloor Controlled-Source Electromagnetic System for Shallow Seabed Characterization

Roslynn B. King, Steven Constable, Jillian M. Maloney, and Amy E. Gusick

***Abstract*—Development of offshore infrastructure, such as wind farms, requires detailed geotechnical information of the seafloor and the identification of potential hazards, such as shallow hydrocarbons. This information can be supplied by electromagnetic surveys optimized for high-resolution data collection through the use of high source frequencies, short source–receiver offsets, and close proximity to the seafloor. We developed such a system, the compact undersea electromagnetic source instrument (CUESI), which transmits a 10–100 Hz, 2–10 amp current on a horizontal dipole and records three-axis electric field signals at offsets of 10–30 m. Unlike bottom-dragged systems, which cannot be used in protected areas, the CUESI system is neutrally buoyant and is flown 1–3 m above the seafloor, maintaining altitude by buoyancy feedback provided by a short counterweight cable. CUESI is capable of operating at water depths up to 200 m. Tests offshore Santa Barbara, California, demonstrate the capability of the system to detect lateral resistivity changes that are consistent with sediment characteristics observed in coring. Inversions of data over the Santa Rosa Fault resolve the fault trace much more sharply than from a similar system towed on the sea surface. Resistors imaged at the seafloor coincide with tar-like features captured by a camera mounted on the CUESI depressor weight. Based on these tests, CUESI would be a useful tool for offshore development because of its ability to measure lateral changes in seafloor character and detect hazards, such as faults and hydrocarbons.**

***Index Terms*—Electromagnetic (EM) sensing, geophysics, marine controlled source electromagnetic (CSEM), ocean exploration technology, ocean resource exploration systems.**

Received 22 May 2025; revised 18 September 2025 and 12 November 2025; accepted 12 November 2025. This work was supported by the National Center for Preservation Technology and Training – National Parks Service, 2019, through the development and deployment of the CUESI system, under Grant P19AP00140, in part by the National Oceanic and Atmospheric Administration Office of Ocean Exploration under research Grant NA20OAR0110428, in part by the Scripps Seafloor Electromagnetic Methods Consortium, and in part by the Cooperative Agreement between San Diego State University Foundation and the US Department of the Interior, Bureau of Ocean Energy, for collecting core locations, under Grant M15AC00012. *(Corresponding author: Roslynn B. King.)*

Associate Editor: W. Huang.

Roslynn B. King is with the Department of Geophysics, Colorado School of Mines, Golden, CO 80401 USA (e-mail: roslynn.king@mines.edu).

Steven Constable is with the Institute of Geophysics and Planetary Physics within Scripps Institution of Oceanography, University of California San Diego, La Jolla, CA 92093 USA.

Jillian M. Maloney is with the Department of Earth and Environmental Sciences, San Diego State University, San Diego, CA 92182 USA.

Amy E. Gusick is with the Department of Anthropology, Natural History Museum Los Angeles County, Los Angeles, CA 90007-4057 USA.

Digital Object Identifier 10.1109/JOE.2025.3647817

I. Introduction

To MEET increasing global energy demands in a carbon-neutral manner, there is a pressing need for the large-scale development of offshore infrastructure, such as wind farms. The safe and effective development of these offshore projects requires efficient methods for characterizing suitable regions for offshore development, as well as collecting geotechnical data for the engineering of moorings and footings.

While electromagnetic (EM) methods have long been proven effective on land for hazard identification and geotechnical evaluations, the current practice in offshore site assessment relies only on seismic and magnetic methods. While these methods are useful for identifying some seafloor structures and hazards, they lack sensitivity to hydrocarbon seeps and trapped gas and fail to provide critical geotechnical information, such as porosity.

Combining seismic and magnetic methods with EM data will provide a comprehensive and more efficient approach to site assessment studies. A holistic methodology, such as this, is vital for safeguarding the environment and protecting the well-being of individuals impacted by offshore development. Here, we will describe a novel controlled source electromagnetic (CSEM) instrument specifically designed to image the porosity and geology of the upper tens of meters of the seafloor for use in offshore infrastructure site assessment studies.

EM surveys have become an established geophysical approach to study changes in seafloor porosity in a variety of shallow seafloor settings (e.g., [1], [2], [3], [4], [5], [6], and [7]). However, these existing EM systems are dragged across the seafloor and so are limited to seafloor settings that are heavily sedimented (to avoid snag points and damage to the instruments) and lack protected status or sensitive habitats (as dragged systems can adversely affect sensitive habitats and cultural features and landscapes), eliminating many seafloor areas from study. To broaden the range of environments suitable for EM applications, we developed an instrument designed to be towed between 1 and 3 m above the seafloor, thereby minimizing impact on seafloor environments and avoiding potential damage from seafloor topography. This new neutrally buoyant CSEM system, known as the compact undersea electromagnetic source instrument (CUESI), collects both inline and vertical electric field data and improves resolution in the shallow seafloor by emitting higher frequency signals and using shorter source–receiver offsets than previous systems.

This article will detail a case study investigating the sensitivity and resolution of the CUESI system in the Southern California Bight and present preliminary results. The goal of this work is to develop a new EM tool for imaging resistivity of the shallow seafloor, which is relevant to offshore infrastructure projects and hazard identification projects.

II. Depth of Sensitivity and Resolution of Deep-Towed EM Systems

The depth of sensitivity and intrinsic resolution of marine CSEM surveys are dependent upon both parametric (variable frequency) and geometric (variable source–receiver spacing) characteristics. The length scale at which electric and magnetic fields decay in a uniform conductor is governed by the skin depth (1) [8]. Skin depth (z_s) is the depth over which EM field amplitudes are reduced by 1/e and phase progresses 1 radian in a uniform conductive medium, σ, and is dependent upon the period of the transmitted signal, T

$$z_s = \sqrt{\frac{T}{\pi \sigma \mu_o}} \tag{1}$$

where μ_o is the permeability of free space. From this equation, one sees that higher frequency energy samples shallower seafloor, whereas lower frequencies are sensitive to deeper depths. Thus, to enhance sensitivity to the shallow subseafloor, higher frequencies should be used. Resolution, on the other hand, is primarily controlled by geometric factors, such as source–receiver offset. Short offsets enable dense data collection and result in high signal-to-noise ratios and so are preferable if the goal is to collect higher resolution profiles of the shallow section of the subseafloor. In addition, short source–receiver offsets facilitate the use of fixed offset towed systems, which significantly simplify surveying logistics.

Higher frequency signals attenuate quickly in conductive seawater, so close proximity of the source and receivers to the seafloor is necessary to maximize coupling. Proximity to the seafloor is also important to maintain resolution achieved from short source–receiver offsets. Therefore, we initially considered a fixed offset bottom-dragged CSEM system with a small array size (<100 m). This not only improves sensitivity in the upper section of the subseafloor but also improves the accuracy of estimating the resistivity of shallowly buried targets or structures [9].

Fixed offset, bottom-dragged systems have been developed over the past three decades to characterize and map the top tens of meters of the seafloor to study a range of targets from groundwater discharge to gas hydrates (e.g., [1], [2], [3], [6], and [7]). However, as these systems are dragged across the seafloor, their use is limited to seafloor settings that are heavily sedimented and without protected status. This limitation can significantly restrict potential survey areas, as nearly 41% of U.S. marine waters are classified as protected. Many offshore infrastructure projects require an assessment study of a planned development area during which the environment should not be significantly altered. Thus, an EM system with minimal impact on the seafloor is essential for surveying in these scenarios and regions. To investigate the shallow subseafloor in protected areas (e.g., marine protected regions, national parks, and cultural heritage sites) or beneath regions with rocky or variable benthic habitats, an EM system would need to limit contact, while not losing sensitivity, with the seafloor.

Limiting contact by "flying" the system over the seafloor has the added benefit of being able to collect vertical electric field data, which are particularly sensitive to changes in near-seafloor resistivity variations [10]. While vertical fields could, in theory, be measured by dragged systems, doing so introduces significant challenges. Vertical electric field measurements, using a horizontal electric dipole source, are inherently more susceptible to motion-induced noise than inline horizontal fields [10]. Contact with the seafloor increases the risk of motion-induced noise through variable electrode–seawater contact, frame tilting and rotation, and mechanical vibrations. In addition, maintaining a stable, upright vertical dipole electrode when dragging across variable seafloor topography is mechanically challenging, with such configurations being prone to damage and unable to reliably maintain vertical orientation, particularly in rough or rocky terrain [11], [12]. Flying the system mitigates these issues and reduces the noise introduced to the vertical field component.

The addition of the vertical electric field results in improved resolution of shallow geologic features by increasing sensitivity to vertical resistivity contrasts in the upper tens of meters of the seafloor. Vertical electric field components, in contrast to horizontal field components, which are more responsive to deeper and lateral variations, improve the ability to resolve near-seafloor layering, abrupt transitions, and thin conductive or resistive units. Field tests and modeling studies show that including vertical data reduces model ambiguity and helps sharpen the recovery of shallow targets, such as shell middens, hydrocarbon accumulations, and sedimentary contacts [10], [13].

During preliminary sensitivity tests for this study, much of the sensitivity to a small conductive target, similar to an anthropogenic pile of shell debris, was from changes in vertical electric field amplitude. Consequently, we designed and developed a "flying" fixed offset CSEM system, incorporating three-axis electric field receivers. The design draws inspiration from an impact study examining benthic habitat effects through various towing techniques and designs across diverse seafloor settings [14], [15].

III. Instrument Design

The CUESI system (see Fig. 1) consists of a negatively buoyant control unit (CUESI) followed by three towfish: one transmitter/receiver and two receivers. CUESI is towed at approximately 5 m off the seafloor and doubles as a depressor weight, dampening the effects of variable tow speeds and surface wave action on the vessel and tow cable. The three towfish are designed to fly closer to the seafloor, at 1–3 m altitude, to maximize EM coupling with the geology. CUESI supplies a controlled current to the transmitter towfish, which transmits the current into the seawater through two 10 cm long, 1.5-cm diameter soft copper tubing sections held 2 m horizontally apart on a rigid frame.

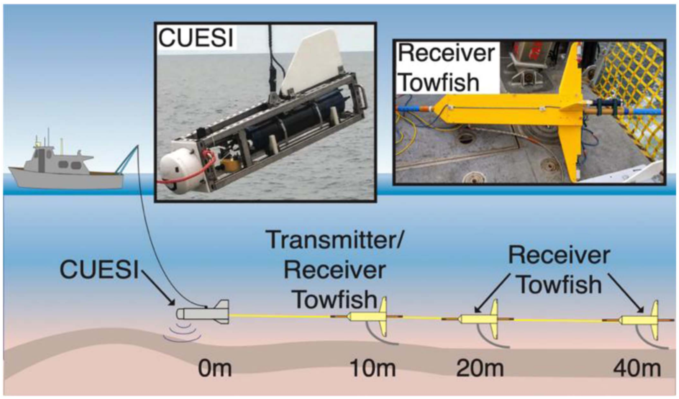

Fig. 1. Schematic of the CUESI array. CUESI is negatively buoyant to act as a depressor weight for the array. All three towfish are trimmed to tow within 3 m of the seafloor. Photos of CUESI and receiver towfish are also pictured.

The two receiver towfish are lightly modified variations of the Vulcan instruments described in [9]. These two receiver towfish record three components of the electric field using orthogonal dipoles: a 2-m dipole for inline (horizontal) fields and 1-m dipole for both crossline and vertical fields. All towfish internally record depth (using Paroscientific pressure gauges) and orientation (pitch, roll, and heading) data, which are internally time stamped, with samples telemetered to the vessel through CUESI at 15-s intervals. CUESI sends a digital signal corresponding to polarity transitions of the transmitted waveform to the towfish, which is recorded on a logger channel at 500 Hz and used in postprocessing to correct for clock drift (which is ∼1 ms/day).

All towfish frames in the array are designed to be positively buoyant and are equipped with a small counterweight in the form of a short cable (i.e., 2 m long, 11.1 mm outside diameter vinyl-jacketed stainless-steel cable) attached to the base of each frame. This cable weighs approximately 0.57 kg, and that ensures when it touches the seafloor, the overall buoyancy of the towfish becomes neutral, allowing the frame to maintain a distance of 1–3 m above the seafloor. While the counterweight cable may make brief contact, its footprint is minimal, and the design is intended to reduce disturbance. This configuration was selected based on prior studies comparing the impact of near-seafloor towed survey systems, where neutrally buoyant, cable-tethered towed platforms were found to be among the least invasive methods available across varied substrate types and benthic habitats, particularly in areas with sensitive biota or cultural features [14], [15].

In developing this configuration, we considered other depth-control approaches that would avoid any seafloor contact but ultimately found them impractical for our deployment conditions. For instance, we tested active hydrodynamic depth control using wings, similar to those used for seismic streamers, but the slow tow speeds (1–2 kn) required for dense spatial coverage, for improved signal-to-noise in high-frequency data, and to maintain a steep cable angle prevent the wings from generating enough vertical lift to overcome array drag. In addition, safely towing within 5 m of the seafloor requires real-time feedback from altimeters rather than pressure gauges used to control depth. However, altimeter data streams are prone to dropouts and signal artifacts, making them unreliable for continuous altitude control. These limitations preclude the use of closed-loop active control in most near-seafloor environments, reinforcing the need for a passively stable system design for this application.

The preliminary data described in the following were collected with the transmitter towfish 10 m behind CUESI and the receiver towfish 10 and 30 m behind the transmitter, using a 25 Hz 2.5–2.8 A square wave transmission.

The development of the CUESI system was initially driven by a study to locate submerged cultural sites (shell-bearing deposits) created by maritime-adapted people living on the now submerged Pleistocene landscapes of the Northern Channel Islands. The primary research goals aimed to characterize landscapes that may contain these submerged sites in a range of water depths from 5 to 110 m. Consideration for vessel capabilities in navigating these shallow waters influenced CUESI's design, accounting for the expected limited deck space and the use of standard 110 VAC power supplies compatible with small (∼13 m long), nonspecialized vessels.

The system's development occurred at the Scripps Marine Electromagnetic Laboratory, which also engineered the "Vulcans"—three-axis electric field receivers [10], [16], [17]. The modified Vulcan receivers that form part of the CUESI array were adjusted for buoyancy and affixed with counterweight cables, and the gain on the loggers was reduced to avoid signal saturation due to reduced source–receiver distances. The transmitter towfish was further altered to function as a mount for the horizontal electric dipole and to only record the vertical electric field with a nominal gain of one on a set of stainless-steel electrodes.

For brevity, this article primarily focuses on the latest iteration of the CUESI system, whereas further details on its iterative development and initial tests are described in separate reports [18], [19].

A. *CUESI Hardware*

CUESI, pictured in Fig. 2, is 140 cm long, 23 cm wide, and 60 cm in height (including the tail wing; 31 cm without wing). The stainless-steel frame weighs approximately 65 kg in air and is outfitted with handles at the front and aft of the instrument to simplify recovery and deployments. The frame is attached to the tow cable slightly aft of center so the instrument will have minimal pitch when towed through the water. The frame is open-sided to reduce drag in the water and provide ease of access to the instrumentation. A camera in a pressure case on a pivot bar, an LED light, a conductivity/temperature sensor, an altimeter, a depth sensor, and control electronics housed in a pressure case are all mounted inside the CUESI frame.

Power and communications from the surface vessel are transmitted to CUESI through an electromechanical cable with a single coaxial conductor. 110 VAC power is provided by the topside control electronics, and a frequency shift keyed communication system overlain on the power allows commands and data to be transmitted up and down the tow cable at 30 characters per second. Within CUESI, a 110 VAC power

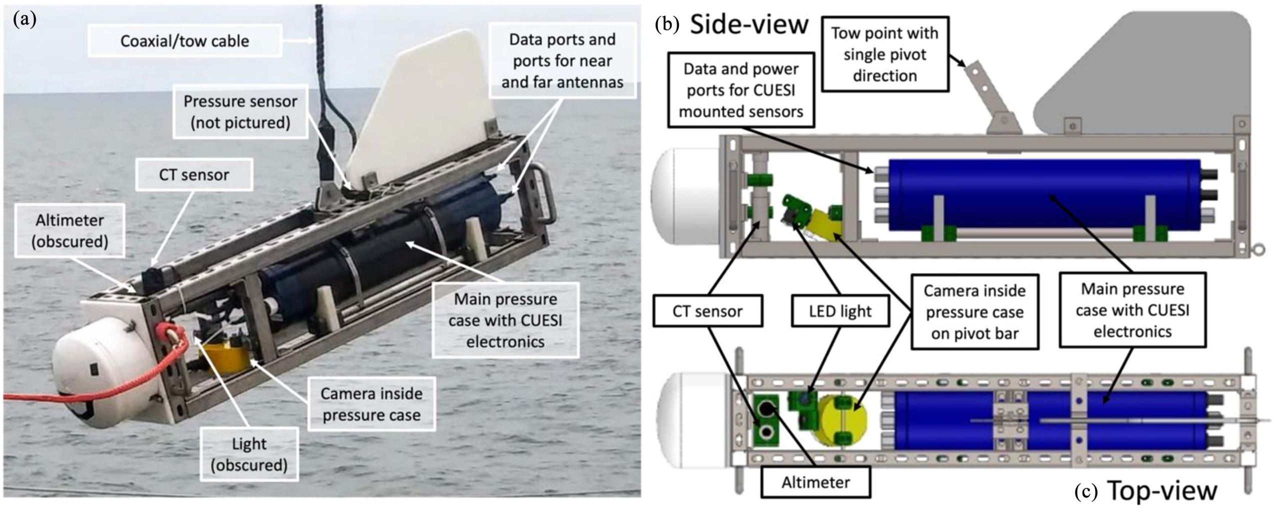

Fig. 2. (a) Photograph of CUESI during pier tests with sensors and frame-mounted instruments labeled. The pressure sensor was not attached during this test, but the location of the sensor is indicated. (b) Schematic of the side-view of CUESI. (c) Schematic of the side view of CUESI. (d) Schematic of the top view of CUESI. The white cap on the front of the frame protects internal sensors and instrumentation from impact with debris and the seafloor.

supply provides 12 VDC, which is then current controlled and switched under computer control to provide arbitrary binary or ternary waveforms. Waveform switching is in increments of 1/2000 s time units. The timing of the waveform is controlled by internal CUESI software using specifications provided by topside commands. An internal oscillator/clock is synchronized to GPS time before launch and maintained by an internal battery to avoid timing disruption associated with power interruption. CUESI outputs a current-controlled waveform of up to 10 amps on the 2-m horizontal electric dipole mounted on the transmitter towfish.

B. Real-Time Data and CUESI Performance

The whole CUESI array is designed to operate within 5 m of the seafloor, necessitating real-time navigation data across the full instrument array to prevent collisions with the seafloor.

All three towfish transmit data, including depth sensor readings, time, pitch, roll, and heading, to CUESI using the RS422 multidrop protocol described in [10]. Once received by CUESI, this information is integrated into the data stream sent topside, including information from sensors affixed to CUESI (altitude readings, output current and voltage, sea temperature, water conductivity, and time).

CUESI and all towfish measure depth to a fraction of a decimeter at 1-s intervals using pressure sensors. While the vessel measures full water depth, CUESI employs an altimeter for accurate real-time seafloor distance measurements. Utilizing altimeter and pressure data, depth profiles and towfish altitudes can be calculated. These real-time navigation data allow the operator to adjust CUESI's elevation via winch controls or via tow speeds. When available, vessel-mounted fathometer data (e.g., Minn Kota 50/200 kHz) were also monitored to anticipate changes in seafloor topography and proactively raise CUESI in advance of abrupt changes in depth or mounded features. We found that towing CUESI 2–5 m above the seafloor at speeds

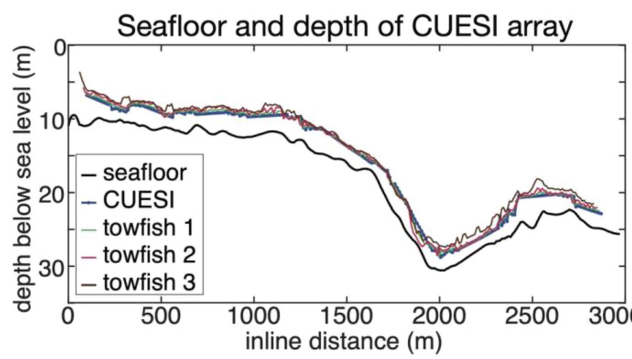

Fig. 3. Plot of the depth of the array while surveying. The towfish generally maintained a distance between 1 and 3 m off the seafloor occasionally reaching 2–4 m due to irregular seafloor features during the survey.

of 1–2 kn gave us enough time to avoid collisions with seafloor irregularities and maintain a towfish altitude of 1–3 m above the seafloor, as shown in Fig. 3.

IV. Case Study

During its development, we tested the CUESI system in several areas offshore Southern California. The location of the case study presented is shown in Fig. 4.

A. Survey Area and Background

The Channel Islands were chosen as a test site for the CUESI system, as sediment core, acoustic reflection, and prior CSEM data are all available in this region. Using the sediment core data, the CUESI system could be tested for its ability to resolve porosity changes within the shallow seafloor. The acoustical reflection profiles were used to provide context for the core locations and lateral constraints on the local geology. In addition, the resolution and sensitivity of the CUESI system could be compared to an existing CSEM system, the Porpoise system

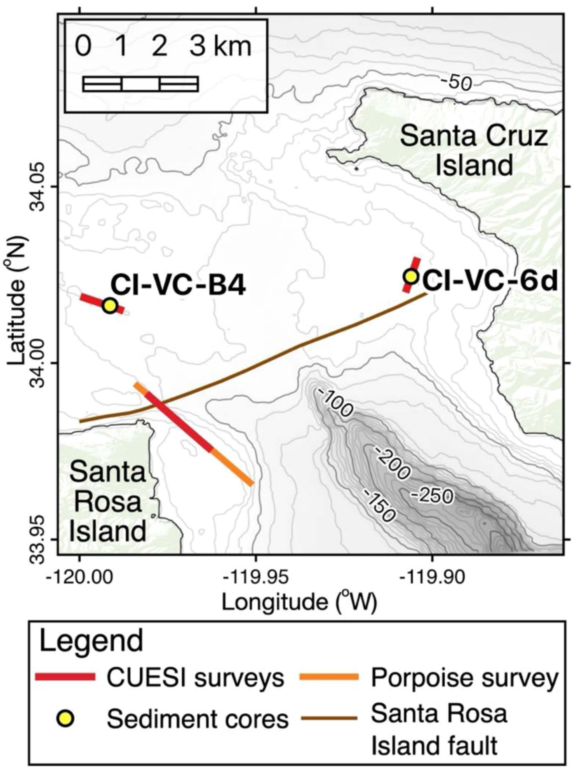

Fig. 4. Case study survey area offshore Southern California. Sediment cores (yellow dots) with CUESI surveys (overlain red lines) are plotted. The porpoise survey (orange) and CUESI survey (red) used in the inversions shown in Fig. 5 are plotted.

[20], in this region. Results comparing the ability of the CUESI system to detect the porosity of the sediment core data are not discussed here, as it was an early test of the system with poor navigational and phase control. A discussion of these first tests can be found in publicly available reports [13], [18]. The case study discussed here uses data from the most current version of the CUESI system, which has improved navigation and produces data with higher signal-to-noise ratios than from prior surveys. These data could be inverted for direct comparison of resistivity models resulting from an existing CSEM system and the CUESI system.

The CUESI system was used to resurvey a profile collected using Porpoise, a surface-towed CSEM system [20]. This survey, as shown in Fig. 4, aimed to image the Santa Rosa Island Fault in water depths of 9–35 m, and identified several resistive features. The CUESI system was towed within 1–4 m of the seafloor at 1–2 kn for 45 min, resulting in data collected over ∼2350 m of seafloor. Concurrently, the camera mounted to the CUESI frame captured seafloor images every 3 s, some of which are shown in Fig. 5.

B. Data Processing and Inversion Methodology

Amplitude and phase data of the CSEM response functions from the second and third towfish were extracted from the electric time-series data using a method detailed by Myer et al. [21]. The resulting transfer function estimates were stacked using a block arithmetic mean over nonoverlapping 10-s intervals to enhance signal-to-noise ratio, providing amplitude and phase response data as a function of position and frequency for the last two towfish. Due to the impact of navigational error on amplitude data at short source–receiver offsets, only phase data from the second towfish (a 10-m source–receiver offset) were included in the inversion. Utilizing the first and third harmonics (25 and 75 Hz), the resulting CUESI survey profile shown in Fig. 5 used a total of 1446 CSEM data. These data were degraded by a 5% error floor to account for navigational uncertainties and then included in the inversion as finite-length dipoles.

The modeling software used in this study is the publicly available, goal-oriented, adaptive, finite-element 2-DMARE2DEM inversion and modeling code [22]. This code uses Occam's Inversion, a method that regularizes the inversion to obtain the smoothest resistivity model that fits the data to a specified misfit [23]. The starting model included the seawater as a fixed parameter, using conductivity data collected by CUESI. The bathymetry profile used in the starting model was generated by combining the depth and altimeter data, also collected by CUESI. Using this model structure, the free parameter region was reduced to the area below the seafloor and set to a uniform starting resistivity of 1 Ωm. An inversion parameter grid was constructed using 10-m-wide quadrilateral cells that increased in height with depth to mimic the loss of resolution of the EM method. Intrinsic to the adaptive nature of the MARE2DEM code, the computation mesh was allowed to refine where necessary to produce accurate responses. The resistivity inversion was run until the final inversion model response converged to a root-mean-square misfit of 1, resulting in the final resistivity profile, labeled "CUESI Profile," depicted in Fig. 5.

The surface-towed CSEM data, obtained using the Porpoise CSEM system [20], were collected nearly two years before the CUESI survey in January 2019 [24], using a 2 Hz, 30-amp waveform-D [21] transmission current on a 10-m antenna, with receivers at 200- and 300-m source–receiver offsets. These data were processed using the same method used for the CUESI data; however, stacking windows were 30 s to account for conditions characteristic of a surface-towed survey. Waveform-D results in a broader range of high-amplitude harmonics than a square wave, and amplitude and phase data for 6, 14, and 26 Hz were included in the inversion for both surface-towed receivers. The amplitude data were subjected to a 2% error floor, and the phase data were subjected to a 1% error floor before being included in the model as finite-length dipoles. The surface-towed CSEM array was towed at a rate of 3–4 kn, which when combined with 30-s stacking windows results in samples every 45–60 m along the survey line. As with the CUESI profile, MARE2DEM was used to generate inversion models. Here, the starting model included seawater as a fixed parameter, using conductivity data collected by a separate towed instrument in the Porpoise array and available bathymetric data. The free inversion region below the seafloor was set to a uniform starting resistivity of 1 Ωm and parameterized using 20-m-wide quadrilateral cells that increased in height with depth. The resistivity inversion was allowed to run until the final resistivity inversion converged to a root-mean-square misfit of 1. The final resistivity inversion, labeled "Porpoise Profile" in Fig. 5, uses 753 CSEM data. Finally, the central profile in Fig. 5, labeled "Profile from Combined

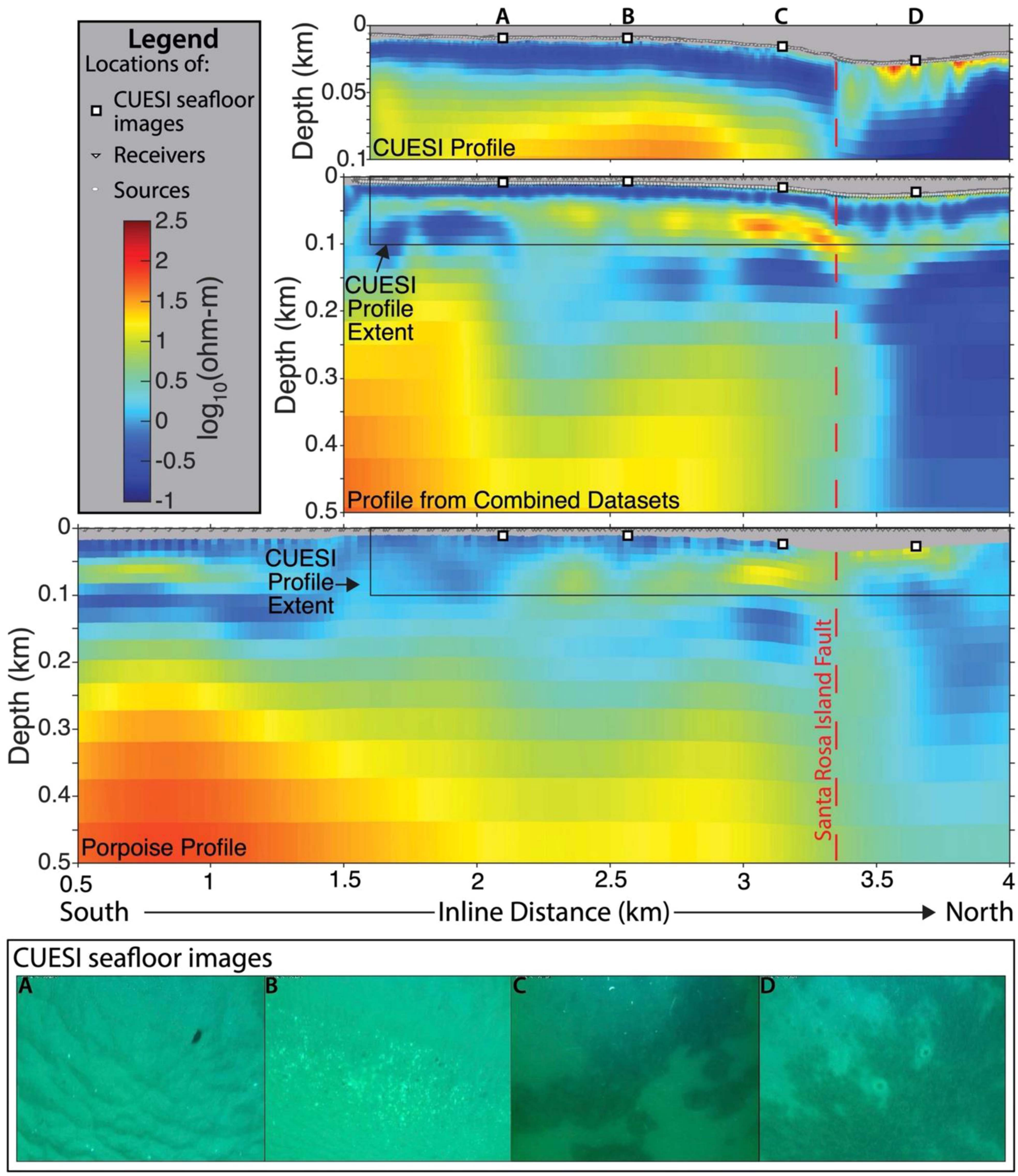

Fig. 5. Resistivity models from the CUESI survey and surface-towed CSEM (Porpoise) survey offshore Santa Rosa Island. The top panel, labeled "CUESI Profile," is a resistivity model from the red survey line shown in Fig. 4. The location of the CUESI profile is marked by a black box on the middle panel. The middle panel, labeled "Porpoise Profile," is a resistivity model from the surface-towed CSEM survey mapped as an orange line in Fig. 4. Warm colors indicate high resistivity and cool colors indicate conductors in both resistivity profiles. The black and white circles and triangles in both profiles mark the locations of the transmitters and receivers used in the modeling code. The black squares on both the top and middle panels are the locations of the photos captured by the CUESI system and shown in the bottom panel.

Datasets," is the result of a joint inversion of both data sets using the same parameters described above. The CUESI profile extent is delineated with a black box, overlaid on the Porpoise profile.

The MARE2DEM code used to generate these profiles computes a sensitivity from the Jacobian derivative matrix by normalizing the Jacobian by data errors and summing the absolute values over all data. This sensitivity vector is then normalized by each parameter area, resulting in a final sensitivity unit of $\log_{10}(\text{S/m})/\text{m}^2$. The $-3.5 \log_{10}(\text{S/m})/\text{m}^2$ sensitivity contour has been observed to correspond to the depth of diminishing sensitivity [9]. The extent of the profiles presented here is limited to the average depth of this contour.

C. Comparison With Existing Surface-Towed CSEM System

There is good agreement between the Porpoise and CUESI resistivity models shown in Fig. 5, particularly to the right of the Santa Rosa Island Fault, where resistivity features align well. However, the CUESI model more sharply delineates the Santa Rosa Island Fault trace than the smoother representation from the Porpoise data. In the CUESI model, the fault clearly laterally separates a more conductive layer over a resistor to the south of the fault from a resistor over a conductor to the north. This general resistive structure is resolved but smoothed in the Porpoise profile. At depth, the fault appears to be collocated with a vertical resistor in the Porpoise profile, possibly indicating resistive fluid migration, such as freshwater or hydrocarbons, up the fault.

The joint inversion shown in Fig. 5 resolves the discrepancies observed in the individual data set inversions, particularly the difference in resistivity at 1.5–2 km inline distance. In this region, the joint inversion reveals a resistor underlain by a conductor—a feature not distinctly present in either the CUESI or Porpoise profiles. One possible explanation is that the CUESI system, due to its limited depth sensitivity, is unable to fully resolve the base of the shallow resistive lens identified in the joint inversion. However, the top of this resistor is within the depth of sensitivity and is resolved in both the CUESI and joint inversion resistivity profile. Conversely, while the Porpoise system provides greater depth sensitivity, the spacing of its receivers and the frequencies used in the survey may have caused this feature to be averaged into an indistinct moderate conductor.

The use of both CUESI and Porpoise data sets in a single inversion reduces ambiguity and produces a geologically plausible resistivity model, particularly where individual surveys may have been limited by resolution and depth of sensitivity tradeoffs. Overall, the CUESI system demonstrates enhanced resolution of subseafloor resistivity due to its shorter source–receiver offsets, proximity to the seafloor, and use of higher source frequencies. This design improves sensitivity to shallow seafloor resistivity variations but significantly reduces the depth of sensitivity compared to the Porpoise system. The joint inversion mitigates these tradeoffs, leveraging the depth sensitivity of the Porpoise system while maintaining the near seafloor (<100 m) lateral resolution of CUESI system.

D. Geologic Interpretation and Refinement With CUESI System

Hydrocarbon accumulations have been documented on nearby beaches [25], suggesting that the resistors along the fault might be tar. This interpretation is supported by the photos captured by the CUESI system during the survey, shown in the bottom panel of Fig. 5 and with locations marked with black squares on both the CUESI and Porpoise profiles. In photos A and B, the seafloor appears to be made up of sand with several sparse accumulations of fractured shells. Here, the seafloor resistivity in the CUESI profile is approximately 1 Ωm, typical of marine sediment with saline pore fluids. The location of photo C marks the southern edge of a 10 Ωm seafloor resistor in the CUESI profile and corresponds to the first occurrence of dark material in the photo series. Photo C is similar to photos taken offshore Point Conception in California and offshore Angola of known tar/asphalt accumulations [25], [26], and combined with the resistivity strongly suggests the presence of seafloor tar accumulations here. The profile from the surface-towed Porpoise data also includes a resistive feature at the seafloor in this approximate location.

Further north along the towlines, photo D is located above a stronger resistor (>30 Ωm) in the CUESI profile and captures a dark patchy seafloor. This photo is consistent with other photos taken between 3.5 and 3.7 km along the towline, the approximate span of the seafloor resistor, and suggests that the seafloor sediment is saturated with hydrocarbons. This type of hydrocarbon accumulation is associated with hydrocarbon seeps that may become temporarily sealed or slowed due to changes in sea state or reservoir pressure [27]. The resistor and darkly colored seafloor extend from the photo C location until approximately 3.85 km along the towline, at which point the seafloor resumes a ∼1 Ωm resistivity in the Porpoise profile and resembles the seafloor captured in Photos A and B.

While hydrocarbons in sediment and active seeps provide a likely explanation for some of these resistive anomalies, an alternative interpretation is that these resistors may also be associated with bedrock, such as the nearby Beechers Bay Formation or Monterey Shale. Generally, these formations are pale in color [28]; however, discoloration from seaweed or other biomass could account for the darker coloration observed in the seafloor images. Alternatively, the Beechers Bay Formation also contains a dark gray, crudely bedded volcanic conglomerate breccia, which is the closest onshore outcropping bedrock to the survey and is consistent with the seafloor photos captured during the survey. The conductive sediments surrounding these resistors likely represent modern seafloor deposits and possibly Quaternary dune and drift sands, as observed at nearby Skunk Point [28], [29]. However, given that outcropping volcanic formations or shales would generally produce a thicker, resistive signature, and considering that the joint inversion notably thins the near-seafloor resistor north of the fault—a characteristic more consistent with tar accumulations—this refinement supports the tar interpretation.

If, on the other hand, these seafloor resistors are indeed bedrock outcrops, the source of the vertical resistor coincident with the Santa Rosa Island Fault remains an open question. Permeability studies onshore suggest that where the Santa Rosa Island Fault is juxtaposed with volcanic rocks, surface water expression is common [30]. Based on these findings, the vertical resistors could represent freshened groundwater traveling up the fault line, consistent with freshwater springs observed along the shoreline at Skunk Point in 2015 [31].

Although the geology of the region remains inconclusive, the CUESI system's improved resolution and ground-truthing capabilities have allowed for a more informed interpretation of the features resolved in the profiles. By providing higher resolution data, CUESI has helped reduce some of the nonuniqueness inherent to EM methods, enabling a more refined geological discussion.

E. Shallow Porosity Imaging

To test the ability of the CUESI system to detect changes in seafloor porosity, the apparent resistivity values from the CUESI

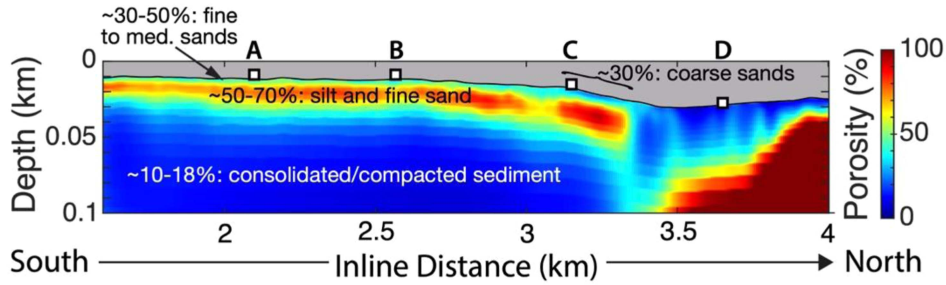

Fig. 6. Porosity profile generated from CUESI resistivity profile using the Humble formula. Porosity values are plotted on a linear scale and spatial dimensions of Fig. 6 match those of the CUESI profile shown in Fig. 5. For the porosity calculations, the pore fluid resistivity is assumed to be 0.245 Ω·m (based on seawater conductivity measured by the CUESI drop weight at time of surveying), *a* is set to 0.62, and *m* is set to 2.

profile shown in Fig. 5 were converted into porosity values using a variation of Archie's law, known as the Humble formula (2) [32]. The Humble formula is commonly used for unconsolidated sediments or loose formations, such as marine sands [32], [33], [34], and is given by the equation

$$\rho_o = a\rho_f\phi^{-m} \tag{2}$$

where ρ_o is the bulk resistivity of the water-saturated material, ρ_f is the resistivity of the pore fluids, ϕ is the porosity of the material, and m is the cementation factor, a measure of how the resistivity of a rock changes with permeability assuming that the pore fluids are more conductive than the grains. The Humble formula uses a constant cementation exponent, m, of 2.15 and a tortuosity factor, a, of 0.62.

The resulting porosity profile, as shown in Fig. 6, is not directly ground-truthed but is broadly consistent with known depositional sequences in the region and published porosity trends in continental shelf sediments (e.g., [3], [35], [36], and [37]), particularly south of the Santa Rosa Fault, which intersects the profile at the 3.35 km inline distance.

Porosity values range from 10% to 18% at depth, increasing to 50%–70% at intermediate depths, and then tapering to 30%–50% nearer the seafloor. These trends are consistent with a basal compacted or lithified unit overlain by fine to very fine marine sediments, interpreted here as a Holocene high stand package or prograding marine deposits [37], [38]. A sharp transition in porosity at 30–40 m depth is interpreted as the transgressive surface, consistent with the location of the transgressive boundary identified by Laws et al. [37]. Although others have mapped a ~0.5–2 m-thick transgressive unit above this boundary [37], it cannot be resolved in this profile due to the resolution possible with the EM method at this depth.

While uncertainties remain in the absolute porosity values due to assumptions in pore fluid resistivity (0.245 Ω·m value was used in these calculations consistent with conductivity measurements recorded with the CTD sensor on the CUESI depressor during the survey) and parameter choice for Archie's law, the exercise demonstrates the utility of CUESI for high-resolution mapping of lateral and vertical porosity trends.

CSEM methods are prone to overfitting conductive features, and this may be the reason for the unnaturally high porosity values north of the fault, located at 3.35 km inline distance. As the same feature is also observed, but to a lesser degree, in Porpoise resistivity profiles, this suggests that the feature is not an artifact, but that the conductivity is a result of overfitting or edge effects. In addition, above this high porosity feature, rocks and/or potential hydrocarbons were observed in the photos, which would make the Humble formula assumption inappropriate. However, if known lithologies (e.g., clays or hydrocarbons) are present, models, such as the Glover–Hole–Pous formulation, could be used in future work to better account for multiphase conduction [34].

V. Conclusion

Although the initial tests of the CUESI system are promising, the system remains in the early stages of development. Our results indicate that the CUESI system is effective at detecting relative changes in seafloor porosity, providing valuable insights into sediment heterogeneity. However, further testing is needed to enable statistical analysis of the system's accuracy at resolving near seafloor porosity values, particularly in its updated form and with improvements to the navigational components to reduce the error floor and further calibration. In addition, tests of CUESI over a variety of seafloor types will better characterize the sensitivity and resolution of the system. Further development to ruggedize the system will streamline data collection, and the incorporation of additional sensors, such as a magnetometer, would transform the system into a multiphysics platform and reduce ambiguity in seafloor characterization.

Despite its current limitations, the CUESI system exhibits improved resolution in characterizing the upper tens of meters of the seafloor when compared to an existing surface-towed CSEM system. This heightened resolution, particularly in assessing pore fluids, holds significant potential for applications in offshore infrastructure projects, such as wind farms, where geotechnical evaluations, including sediment stratigraphy and porosity, are crucial for the design and secure installation of structures. Moreover, the CUESI system is nondestructive, minimizing impact on the seafloor, which makes it an attractive new tool to survey paleolandscapes that were subaerial during times relevant to human occupation or in regions with unmapped or sensitive benthic communities. Traditional site assessment methods, such as subbottom acoustical profilers, can be used concurrently with the CUESI system, creating a more efficient and holistic approach to site assessment.

Acknowledgment

The authors are grateful for John Soulders, Chris Armerding, and Jake Perez of the SIO EM Laboratory for their tireless efforts and patience in the design, build, modification, and deployments of the CUESI system. In particular, the authors would like to acknowledge John Soulders for his exceptional work on the CUESI transmitter hardware, which was a significant undertaking and helped make this project possible. The authors would also like to thank the Captain, Brett Pickering, of the RV Bob and Betty Beyster who enthusiastically helped collect all the data discussed here. The authors extend their gratitude to Andrew Mendoza and Eva Pagaling for their valuable assistance in data collection and for generously sharing their cultural insights related to the Channel Islands.

References

[1] S. Cheesman, L. Law, and B. S. Louis, "A porosity mapping survey in Hecate Strait using a seafloor electro-magnetic profiling system," *Mar. Geol.*, vol. 110, no. 3/4, pp. 245–256, Mar. 1993.

[2] R. L. Evans, "Measuring the shallow porosity structure of sediments on the continental shelf: A comparison of an electromagnetic approach with cores and acoustic backscatter," *J. Geophys. Res.*, vol. 106, no. C11, pp. 27047–27060, 2001.

[3] R. L. Evans, "Using CSEM techniques to map the shallow section of seafloor: From the coastline to the edges of the continental slope," *Geophysics*, vol. 72, no. 2, 2007, doi: 10.1190/1.2434798.

[4] R. L. Evans, L. Law, B. St Louis, S. Cheesman, and K. Sananikone, "The shallow porosity structure of the Eel shelf, Northern California: Results of a towed electromagnetic survey," *Mar. Geol.*, vol. 154, no. 1–4, pp. 211–226, Feb. 1999.

[5] A. Micallef et al., "3D characterisation and quantification of an offshore freshened groundwater system in the Canterbury Bight," *Nat. Commun.*, vol. 11, no. 1, pp. 1–15, Dec. 2020, doi: 10.1038/s41467-020-14770-7.

[6] K. Schwalenberg, M. Haeckel, J. Poort, and M. Jegen, "Evaluation of gas hydrate deposits in an active seep area using marine controlled source electromagnetics: Results from Opouawe Bank, Hikurangi Margin, New Zealand," *Mar. Geol.*, vol. 272, no. 1–4, pp. 79–88, Jul. 2010, doi: 10.1016/j.margeo.2009.07.006.

[7] K. Schwalenberg, E. Willoughby, R. Mir, and R. N. Edwards, "Marine gas hydrate electromagnetic signatures in Cascadia and their correlation with seismic blank zones," *First Break*, vol. 23, no. 4, pp. 57–63, Apr. 2005, doi: 10.3997/1365-2397.23.4.26501.

[8] H. A. Wheeler, "Formulas for the skin effect," *Proc. IRE*, vol. 30, pp. 412–424, Sep. 1942, doi: 10.1109/JRPROC.1942.232015.

[9] R. B. King and S. Constable, "How low can you go: An investigation of depth sensitivity and resolution using towed marine CSEM systems," *Geophysical Prospecting*, vol. 71, no. 4, pp. 722–733, Apr. 2023, doi: 10.1111/1365-2478.13345.

[10] S. Constable, P. K. Kannberg, and K. Weitemeyer, "Vulcan: A deep-towed CSEM receiver," *Geochemistry, Geophys., Geosystems*, vol. 17, no. 3, pp. 1042–1064, Mar. 2016, doi: 10.1002/2015GC006174.

[11] S. Constable, "Review paper: Instrumentation for marine magnetotelluric and controlled source electromagnetic sounding," *Geophysical Prospecting*, vol. 61, no. SUPPL.1, pp. 505–532, Jun. 2013, doi: 10.1111/j.1365-2478.2012.01117.x.

[12] B. S. Singer, "Far-zone fields of electric and magnetic dipoles in a stratified laterally isotropic Earth and mitigating the airwave in marine CSEM," *Geophysical J. Int.*, vol. 201, no. 3, pp. 1568–1597, Mar. 2015, doi: 10.1093/gji/ggv119.

[13] A. Gusick, J. Maloney, S. Constable, T. Braje, K. Hoppa, and R. King, "Using controlled source electromagnetic methods for detecting submerged archaeological resources," National Center for Preservation Technology and Training (NCPTT), NPS NCPTT Grant: P19AP00140, Dec. 2021, pp. 1–24. Accessed: Jan. 31, 2025. [Online]. Available: https://rozbking.github.io/pdfs/FinalReport_2021_NHM_P19AP00140_1.pdf

[14] E. V. Sheehan et al., "An experimental comparison of three towed underwater video systems using species metrics, benthic impact and performance," *Methods Ecol. Evol.*, vol. 7, no. 7, pp. 843–852, Jul. 2016, doi: 10.1111/2041-210X.12540.

[15] E. Sheehan et al., "A comparative study of towed underwater video methodology to monitor benthic habitats in marine protected areas," INTERREG programme France (Channel) England funded project, 2014, pp. 1–46. Accessed: May 01, 2022. [Online]. Available: https://www.panache.eu.com/upload/iedit/10/pj/2145_5698_WP2ENcomparative_study_of_towed_underwater_video.pdf

[16] K. A. Weitemeyer, S. C. Constable, K. W. Key, and J. P. Behrens, "First results from a marine controlled-source electromagnetic survey to detect gas hydrates offshore Oregon," *Geophys. Res. Lett.*, vol. 33, no. 3, pp. 1–4, Feb. 2006, doi: 10.1029/2005GL024896.

[17] K. Weitemeyer and S. Constable, "Mapping shallow geology and gas hydrate with marine CSEM surveys," *First Break*, vol. 28, no. 6, pp. 97–102, Jun. 2010. Available: http://www.researchgate.net/publication/311846345_Mapping_shallow_geology_and_gas_hydrate_with_marine_CSEM_surveys

[18] R. B. King, "Controlled-source electromagnetic studies of the Southern California Continental Shelf," Ph.D. dissertation, Univ. California, San Diego, San Diego, CA, USA, 2022. Accessed: Jan. 04, 2023. [Online]. Available: https://escholarship.org/uc/item/5j24w1ww

[19] A. E. Gusick, J. Maloney, R. B. King, and T. J. Braje, "Emerging technologies in the search for the submerged cultural landscapes of the pacific continental shelf," 2019, doi: 10.4043/29221-MS.

[20] D. Sherman, P. Kannberg, and S. Constable, "Surface towed electromagnetic system for mapping of subsea Arctic permafrost," *Earth Planet. Sci. Lett.*, vol. 460, pp. 97–104, Feb. 2017, doi: 10.1016/j.epsl.2016.12.002.

[21] D. Myer, S. Constable, and K. Key, "Broad-band waveforms and robust processing for marine CSEM surveys," *Geophys. J. Int.*, vol. 184, no. 2, pp. 689–698, Feb. 2011, doi: 10.1111/j.1365-246X.2010.04887.x.

[22] K. Key, "MARE2DEM: A 2-D inversion code for controlled-source electromagnetic and magnetotelluric data," *Geophys. J. Int.*, vol. 207, no. 1, pp. 571–588, Oct. 2016, doi: 10.1093/gji/ggw290.

[23] S. C. Constable, R. L. Parker, and C. G. Constable, "Occam' s inversion: A practical algorithm for generating smooth models from electromagnetic sounding data," *Geophysics*, vol. 52, no. 3, pp. 289–300, 1987, doi: 10.1190/1.1442303.

[24] R. B. King, S. Constable, and J. M. Maloney, "A case study in controlled source electromagnetism: Near seabed hydrocarbon seep systems of coal oil point, California, USA," *Mar. Petroleum Geol.*, vol. 139, May 2022, Art. no. 105636, doi: 10.1016/j.marpetgeo.2022.105636.

[25] T. D. Lorenson et al., "Natural offshore oil seepage and related tarball accumulation on the California Coastline; Santa Barbara channel and the Southern Santa Maria Basin; source identification and inventory," *US Geological Surv. Open-File Rep.*, vol. 1225, pp. 2009–2030, 2009, doi: 10.3133/ofr20091225.

[26] D. O. B. Jones et al., "Asphalt mounds and associated biota on the Angolan margin," *Deep Sea Res. Part I: Oceanographic Res. Papers*, vol. 94, pp. 124–136, Dec. 2014, doi: 10.1016/j.dsr.2014.08.010.

[27] I. Leifer, "A synthesis review of emissions and fates for the coal oil point marine hydrocarbon seep field and California marine seepage," *Geofluids*, vol. 2019, no. 1, pp. 1–48, 2019, doi: 10.1155/2019/4724587.

[28] T. W. Dibblee and H. E. Ehrenspeck, "Geology of Santa Rosa Island, California," in *Proc. 5th California Islands Symp.*, 2002, pp. 115–126, doi: 10.32375/1998-MP45.

[29] T. W. Dibblee, J. J. Woolley, and H. E. Ehrenspeck, "Geologic map of Santa Rosa Island, Santa Barbara County, California," Dibblee Geological Foundation, 1998. Accessed: Jan. 04, 2022. [Online]. Available: https://ngmdb.usgs.gov/Prodesc/proddesc_71695.htm

[30] K. Schmidt and S. Minor, "Surface water availability and field-measured permeability on Santa Rosa Island, Channel Islands National Park, California," in *Proc. AGU Fall Meeting Abstr.*, 2020, pp. H215–003, doi: 10.1002/essoar.10505391.1.

[31] P. Power and R. Rudolph, "Quantifying surface water on Santa Rosa Island, California, following a major five-year drought," *Western North Amer. Naturalist*, vol. 78, no. 4, pp. 530–539, Dec. 2018, doi: 10.3398/064.078.0402.

[32] W. O. Winsauer, H. M. Shearin, Jr., P. H. Masson, and M. Williams, "Resistivity of brine-saturated sands in relation to pore geometry," *AAPG Bull.*, vol. 36, no. 2, pp. 253–277, Feb. 1952, doi: 10.1306/3D9343F4-16B1-11D7-8645000102C1865D.

[33] E. Noaman, "A fast and accurate method for parameter estimation of Archie saturation equation," in *Proc. SPE Middle East Oil Gas Show Conf.*, 1997, pp. 541–553, doi: 10.2118/37744-MS.

[34] P. W. J. Glover, "Archie's law - A reappraisal," *Solid Earth*, vol. 7, no. 4, pp. 1157–1169, Jul. 2016, doi: 10.5194/se-7-1157-2016.

[35] E. Seibold and W. Berger, *The Sea Floor: An Introduction to Marine Geology*, 4th ed. Berlin, Germany: Springer-Verlag, 2017, doi: 10.1007/978-3-319-51412-3.

[36] E. L. Hamilton and R. T. Bachman, "Sound velocity and related properties of marine sediments," *J. Acoustical Soc. Amer.*, vol. 72, no. 6, pp. 1891–1904, Dec. 1982, doi: 10.1121/1.388539.

[37] A. W. Laws, J. M. Maloney, S. Klotsko, A. E. Gusick, T. J. Braje, and D. Ball, "Submerged paleoshoreline mapping using high-resolution Chirp sub-bottom data, Northern Channel Islands platform, California, USA," *Quaternary Res.*, vol. 93, no. 1, pp. 1–22, Jan. 2020, doi: 10.1017/qua.2019.34.

[38] H. W. Posarnentier and G. P. Allen, *Siliciclastic Sequence Stratigraphy—Concepts and Applications*, vol. 7. Tulsa, OK, USA: SEPM Soc. Sedimentary Geol., 1999, doi: 10.2110/csp.99.07.

Roslynn B. King received the B.S. (Hons.) degree in geological engineering from the Colorado School of Mines, Golden, CO, USA, in 2014, and the Joint Ph.D. degree in geophysics from San Diego State University and the University of California San Diego, San Diego, CA, USA, in 2022.

From 2022 to 2024, she was a Postdoctoral Scholar with the Institute of Geophysics and Planetary Physics, University of California San Diego. She is currently an Assistant Professor with the Department of Geophysics, Colorado School of Mines. Her previous professional experience includes serving as an Exploration Geologist for rare Earth elements, a Geotechnical Engineer, and a Physical Scientist with the U.S. Geological Survey. Her research interests include using marine controlled-source electromagnetics for offshore groundwater characterization, archaeological studies, marine seeps, and volcanic hazard assessment.

Steven Constable received the B.S. degree with first class honors in geology from the University of Western Australia, Perth, WA, Australia, in 1979, and the Ph.D. degree in geophysics from the Research School of Earth Sciences, Australian National University, Canberra, ACT, Australia, in 1983.

He is currently a Distinguished Professor of geophysics with the Cecil H. and Ida M. Green Institute of Geophysics and Planetary Physics, Scripps Institution of Oceanography, University of California San Diego, San Diego, CA, USA, where he has held various positions since joining as a Postdoctoral Scholar in 1983. He has led the development and application of robust electromagnetic sensors for offshore exploration. His fleet of broadband electromagnetic sensors has been deployed on the seabed more than 2000 times to map underlying geological structure using variations of both natural magnetotelluric and controlled-source electromagnetic fields. His research interests include subduction zones, offshore volcanic hazards, offshore groundwater resources, geotechnical characterization, geothermal systems, gas hydrate studies, and offshore carbon dioxide sequestration.

Jillian M. Maloney received the B.S. degree in geological sciences from the University of Southern California, Los Angeles, CA, USA, in 2004, and the Ph.D. degree in earth sciences from the Scripps Institution of Oceanography, University of California San Diego, San Diego, CA, in 2013.

She is currently an Associate Professor with the Department of Earth and Environmental Sciences, San Diego State University, San Diego. Following her doctorate, she was a Postdoctoral Researcher with Louisiana State University. Her research combines geophysical data, including seismic reflection, multibeam bathymetry, and sidescan sonar with sediment analysis to understand tectonics and sediment processes on and beneath the seafloor. Her research interests include submarine earthquakes and landslides, offshore neotectonics, and the geologic aspects of marine ecosystems.

Amy E. Gusick received the B.A. degree in communications from Seton Hall University, South Orange, NJ, USA, in 1996, and the M.A. and Ph.D. degrees in archaeology from the University of California, Santa Barbara, CA, USA, in 2007 and 2012, respectively.

From 2015 to 2017, she was an Assistant Professor and Director of the M.A. Program in applied archaeology with California State University, San Bernardino. She is currently the Curator of Anthropology with the Natural History Museum of Los Angeles County, Los Angeles, CA. She uses both terrestrial and underwater archaeological methods to investigate early human coastal migration and settlement along the Pacific Rim. Her research interests include human–environmental dynamics, the development of maritime societies, peopling of the Americas, and maritime cultural landscapes.